



Title	A new zero-voltage-transition converter for switched reluctance motor drives
Author(s)	Ching, TW; Chau, KT; Chan, CC
Citation	The 29th IEEE Power Electronics Specialists Conference Record, Fukuoka, Japan, 17-22 May 1998. In IEEE Power Electronics Specialists Conference Record, 1998, v. 2, p. 1295-1301
Issued Date	1998
URL	http://hdl.handle.net/10722/46087
Rights	©1998 IEEE. Personal use of this material is permitted. However, permission to reprint/republish this material for advertising or promotional purposes or for creating new collective works for resale or redistribution to servers or lists, or to reuse any copyrighted component of this work in other works must be obtained from the IEEE.

A New Zero-Voltage-Transition Converter for Switched Reluctance Motor Drives

T.W. Ching, K.T. Chau and C.C. Chan

Department of Electrical and Electronic Engineering,
The University of Hong Kong, Pokfulam, HONG KONG

ABSTRACT

Firstly, a new zero-voltage-transition (ZVT) converter for switched reluctance motor drives is presented. The proposed ZVT converter possesses the definite advantages that both main transistors and diodes can operate with zero-voltage switching (ZVS), unity device voltage and current stresses. Secondly, its zero-current counterpart is also presented, which offers both the main and auxiliary switches operating with zero-current switching (ZCS) and minimum current / voltage stress. They both have simple circuit topology, minimum component count and low cost. This family of converters is especially advantageous for switched reluctance motor drives demanding efficient regenerative braking, such as electric vehicle application.

1. INTRODUCTION

The switched reluctance motor (SRM) drive is a kind of brushless motor drives, without any rotor conductors nor permanent magnets. The SRM operates on the force of magnetic attraction with the simplest configuration compared with the other types of brushless motors. The SRM drive has some definite advantages for electric vehicle propulsion – simplest and most reliable construction, high efficiency over wide speed and torque ranges, high starting torque and low starting power, fully controllable four-quadrant operation and fast dynamic response.

Within the last decade, the research and development on SRM drives have been focused on the motor topology design and optimization as well as the motor control strategies. Nevertheless, a number of converter topologies for SRM drives have also been proposed [1]. However, most of these converter topologies employ the hard-switching technique which causes high switching losses and severe electromagnetic interference (EMI).

Recently, a number of soft-switching techniques, providing zero-voltage switching (ZVS) or zero-current switching (ZCS) condition, have been successfully developed for switched-mode power supplies (SMPS) [2]-[6]. Surprisingly, the development of soft-switching converters for dc and SRM drives has been very little. Even so, it has been assumed that those being

developed for SMPS can be directly applicable [7]. Until recently, a few studies on soft-switching converters for dc and SRM drives have been carried out [8]-[11].

In this paper, a new soft-switching pulse-width-modulated converter, namely the zero-voltage-transition (ZVT) type, as well as its zero-current counterpart, namely the zero-current-transition (ZCT) type are proposed for SRM drives. This family of converters possesses some definite advantages over its PWM counterpart and other soft-switching converters. For the ZVT converter, ZVS can be achieved for all main switches and diodes, with unity device voltage and current stresses, as well as wide operating range. For the ZCT converter, both the main and auxiliary switches can operate with ZCS and minimum voltage / current stress. They both have simple circuit topology, minimum hardware count, and low cost, leading to achieve high switching frequency, high power density and high efficiency.

Fig. 1 shows the circuit diagram of a conventional hard-switching $(n+1)$ -switch converter for SRM drives. The upper chopping switch S_m serves all three phases while the lower commutating switches S_1 , S_2 and S_3 commutate the phases by selecting one phase at a time sequentially. For example, in Fig. 2(a), phase-1 is selected by turning on S_1 and the phase-1 current is controlled by switching S_m . After a desired time, in Fig. 2(b), S_m is turned off and the phase-1 current is freewheeling by D_m . Then, in Fig. 2(c), S_1 is turned off and energy returns to the source through D_m and D_1 . The SRM can be operated at regeneration simply by retarding the firing angles in such a way that the phase winding conduction period comes after the aligned position.

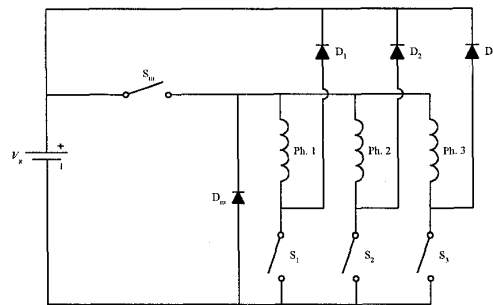


Fig. 1. Conventional converter for SRM drives.

2. PRINCIPLE OF OPERATION OF ZVT-SRM DRIVES

To achieve ZVT operation, two resonant tanks are added to form the proposed ZVT converter for SRM drives shown in Fig. 3. A resonant inductor L_a , a resonant capacitor C_a , an auxiliary switch S_a and a diode D_a are added to the chopping switch S_m . A resonant inductor L_b , three resonant capacitors C_{b1-3} , an auxiliary switch S_b and four diodes D_b and D_{b1-3} are added to the commutating switches S_{1-3} .

A simplified one-phase circuit diagram is shown in Fig. 4. S_m , D_m , V_g and the phase winding can be treated as a buck converter while S_{1-3} , D_{1-3} , V_g and the phase winding can be treated as a boost converter. The equivalent circuits and operating waveforms are shown in Figs. 5 to 8, respectively. As shown in Figs. 5 and 7, there are seven operating stages within one switching cycle, which are briefly described as follows.

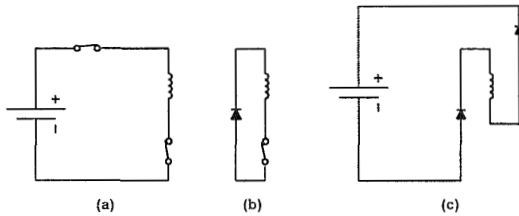


Fig. 2. Conduction modes for one phase.

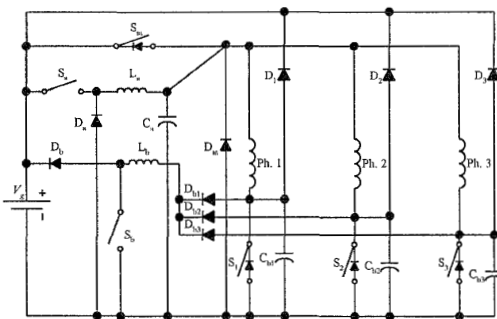


Fig. 3. Proposed ZVT converter for SRM drives.

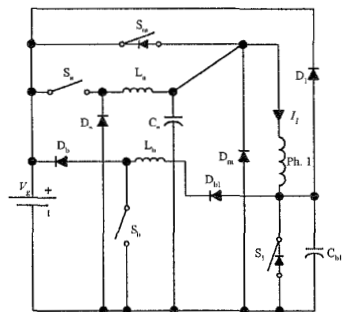


Fig. 4. Simplified one-phase circuit diagram.

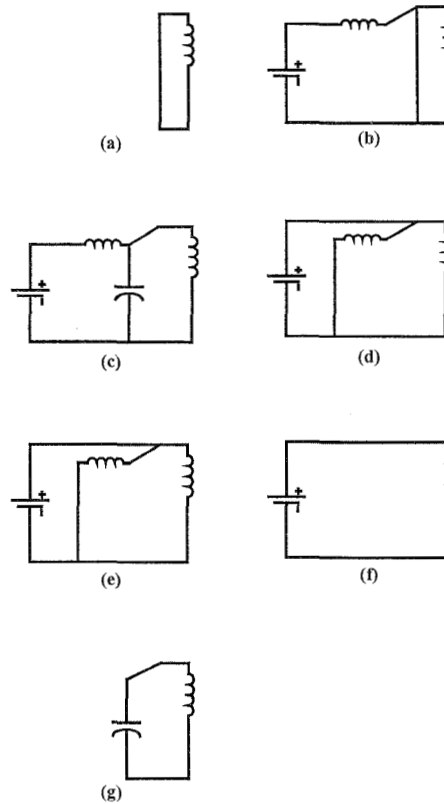


Fig. 5. Equivalent circuit for ZVT operation of S_m and D_m .

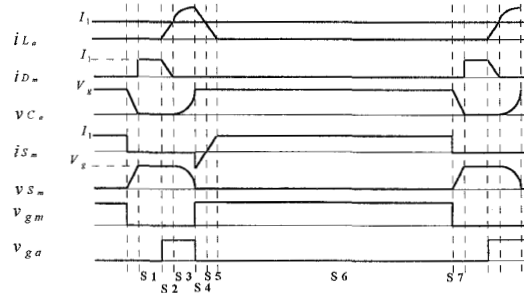


Fig. 6. Key waveforms for S_m and D_m .

2.1 ZVT Operation of S_m and D_m with L_a , C_a , S_a and D_a . (Figs. 5 & 6)

- (a) Stage 1 [T_0 - T_1]: It is a freewheeling mode via D_m .
- (b) Stage 2 [T_1 - T_2]: S_a is turned on. i_{L_a} increases according to the slope of V_g/L_a .
- (c) Stage 3 [T_2 - T_3]: When $i_{L_a}=I_l$, D_m is turned off with ZVS, and L_a and C_a start resonating.

- (d) Stage 4 [T_3 - T_4]: When v_{c_a} reaches V_g , S_m is turned on with ZVS. S_a is turned off to recover the stored energy in L_a to the source. Then i_{L_a} flows through D_a and decreases linearly with a slope of V_g/L_a .
- (e) Stage 5 [T_4 - T_5]: i_{L_a} keeps decreasing while i_{S_m} increasing until i_{L_a} reaches zero at T_5 and D_a becomes off.
- (f) Stage 6 [T_5 - T_6]: It is a powering mode.
- (g) Stage 7 [T_6 - T_7]: I_l discharges C_a linearly with a slope of I_l/C_a until v_{c_a} equals zero at T_7 , and eventually D_m becomes conducting.

2.2 ZVT Operation of S_1 and D_1 with L_b , C_b , S_b , D_b and D_{b1} . (Figs. 5 & 6)

- (a) Stage 1 [T_0 - T_1]: D_1 is conducting, a regenerating mode.
- (b) Stage 2 [T_1 - T_2]: S_b is turned on. i_{L_b} increases with the slope of V_g/L_b .
- (c) Stage 3 [T_2 - T_3]: When i_{L_b} reaches I_l at T_2 , D_1 is turned off with ZVS, and L_b and C_b start resonating.
- (d) Stage 4 [T_3 - T_4]: When v_{c_b} reaches zero, S_1 is turned on with ZVS. S_b is turned off to recover the stored energy in L_b to the source. Then i_{L_b} flows through D_b and D_{b1} and decreases linearly.
- (e) Stage 5 [T_4 - T_5]: i_{L_b} keeps decreasing and i_{S_1} increasing until i_{L_b} reaches zero at T_5 . D_b and D_{b1} becomes off.
- (f) Stage 6 [T_5 - T_6]: It is a freewheeling mode.
- (g) Stage 7 [T_6 - T_7]: I_l charges C_b linearly with a slope of I_l/C_b until v_{c_b} equals V_g at T_7 , and eventually D_1 becomes conducting.

3. PRINCIPLE OF OPERATION OF ZCT-SRM DRIVES

To achieve ZCT operation, two resonant tanks are added to form the proposed ZCT converter for SRM drives shown in Fig. 9. A resonant inductor L_a , a resonant capacitor C_a , an auxiliary switch S_a and a diode D_a are added to the chopping switch S_m . A resonant inductor L_b , a resonant capacitor C_b , a diode D_b , and four auxiliary switches S_b and S_{b1-3} are added to the commutating switches S_{1-3} .

A simplified one-phase circuit diagram is shown in Fig. 10. S_m , D_m , V_g and the phase winding can be treated as a buck converter while S_1 , D_1 , V_g and the phase winding can be treated as a boost converter. The equivalent circuits and operating waveforms are shown in Figs. 11 to 14, respectively.

It should be noted that although the necessary hardware component for achieving the ZCT operation is similar to that for zero-voltage transition (ZVT), their hardware configurations, principles of operation, equivalent circuits as well as operating waveforms and characteristics are very different. As shown in Figs. 11 and 13, there are nine operating stages within one switching cycle, which are briefly described as follows.

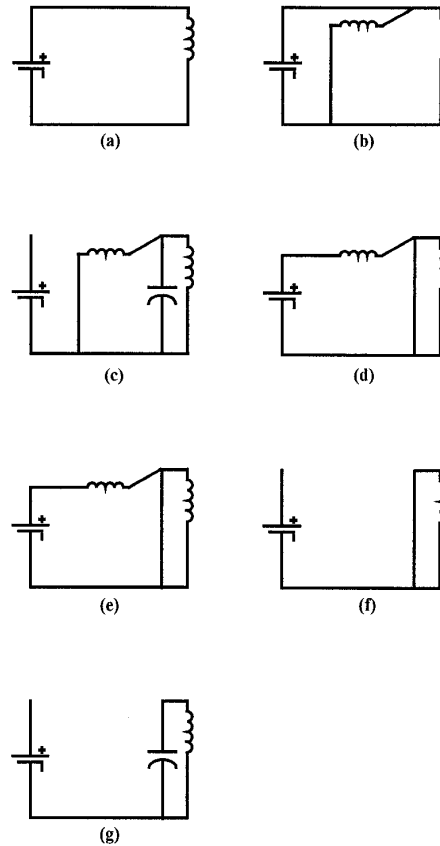


Fig. 7. Equivalent circuit for ZVT operation of S_1 and D_1 .

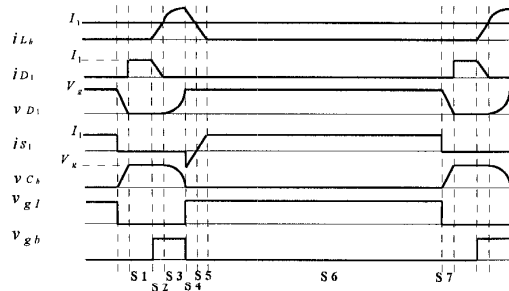


Fig. 8. Key waveforms for S_1 and D_1 .

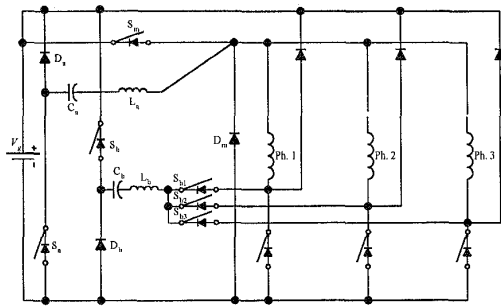


Fig. 9. Proposed ZCT converter for SRM drives.

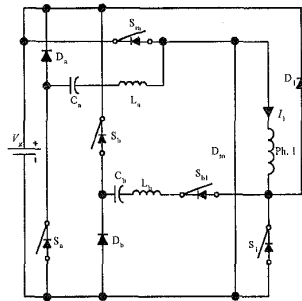


Fig. 10. Simplified one-phase circuit diagram.

3.1 ZCT Operation of S_m with L_a , C_a , S_a and D_a . (Figs. 11 & 12)

- (a) Stage 1 [T_0 - T_1]: S_a is turned on and L_a and C_a start resonating. When i_{L_a} increases from zero to peak and then decreases toward zero and changes direction. i_{L_a} reaches $-I_1$ at T_1 and the antiparallel diode of S_a becomes on.
- (b) Stage 2 [T_1 - T_2]: S_a is turned off and S_m is turned on with ZCS at T_1 . The current of D_m is directed to the auxiliary circuit. i_{L_a} increases rapidly towards zero.
- (c) Stage 3 [T_2 - T_3]: i_{L_a} returns to zero at T_2 and the antiparallel diode of S_a is turned off naturally. L_a and C_a continue resonating and the positive i_{L_a} is conducted by D_a . i_{L_a} returns to zero and D_a is turned off naturally at T_3 .
- (d) Stage 4 [T_3 - T_4]: It is a powering mode.
- (e) Stage 5 [T_4 - T_5]: Before S_m is turned off, S_a is turned on again. L_a and C_a start resonating. When i_{L_a} increases from zero to peak and then decreases toward zero and changes direction and reaches $-I_1$ at T_5 and the antiparallel diode of S_a becomes on.
- (f) Stage 6 [T_5 - T_6]: At T_5 i_{L_a} reaches $-I_1$ and the current of S_m is reduced to zero, so S_m is turned

off with ZCS. As i_{L_a} keeps decreasing, and flows through the antiparallel diode of S_m .

- (g) Stage 7 [T_6 - T_7]: At T_6 , i_{L_a} reaches to $-I_1$ and the antiparallel diode of S_m stops conducting.
- (h) Stage 8 [T_7 - T_8]: At T_7 , v_{C_a} is discharged to zero and D_m starts to conduct. The current in D_m increases gradually.
- (i) Stage 9 [T_8 - T_9]: It is a freewheeling mode via D_m .

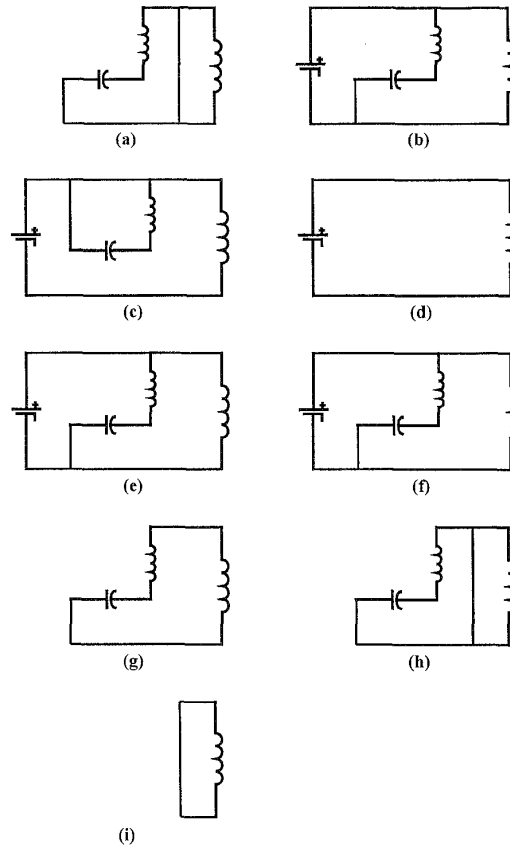


Fig. 11. Equivalent circuit for ZCT operation of S_m .

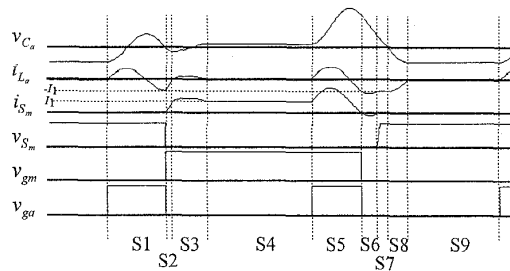


Fig. 12. Key waveforms for S_m .

3.2 ZCT Operation of S_1 with L_b , C_b , S_b and S_{b1} . (Figs. 13 & 14)

- (a) Stage 1 [T_0-T_1]: S_b and S_{b1} are turned on and L_b and C_b start resonating. When i_{L_b} decreases from zero to negative peak and then increases toward zero and changes direction. i_{L_b} reaches I_1 at T_1 and the antiparallel diode of S_b and S_{b1} become on.
- (b) Stage 2 [T_1-T_2]: S_b and S_{b1} are turned off and S_1 is turned on with ZCS at T_1 . The current of D_1 is directed to the auxiliary circuit. i_{L_b} decreases rapidly towards zero.
- (c) Stage 3 [T_2-T_3]: i_{L_b} returns to zero at T_2 and the antiparallel diode of S_b and S_{b1} are turned off naturally. L_b and C_b continue resonating and the negative i_{L_b} is conducted by D_b and D_{b1} . i_{L_b} returns to zero and D_b and D_{b1} are turned off naturally at T_3 .
- (d) Stage 4 [T_3-T_4]: It is a freewheeling mode
- (e) Stage 5 [T_4-T_5]: Before S_1 is turned off, S_b and S_{b1} are turned on again. L_b and C_b start resonating. When i_{L_b} decreases from negative zero to peak and then increases toward zero and changes direction and reaches I_1 at T_5 and the antiparallel diode of S_b and S_{b1} become on.
- (f) Stage 6 [T_5-T_6]: At T_5 reaches I_1 and the current of S_1 is reduced to zero, so S_1 is turned off with ZCS. As i_{L_b} keeps increasing, and flows through the antiparallel diode of S_1 .
- (g) Stage 7 [T_6-T_7]: At T_6 , i_{L_b} falls to I_1 and the antiparallel diode of S_1 stops conducting.
- (h) Stage 8 [T_7-T_8]: At T_7 , v_{C_b} is discharged to zero and D_1 starts to conduct. The current in D_1 increases gradually.
- (i) Stage 9 [T_8-T_9]: It is a powering mode via D_1 .

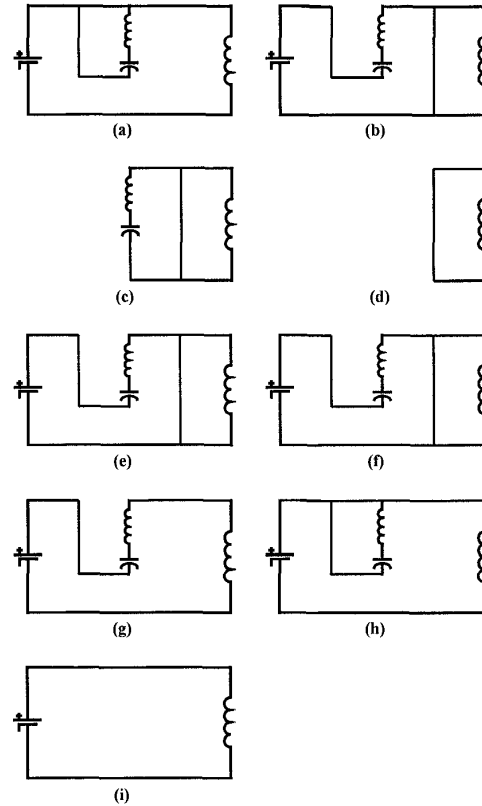


Fig. 13. Equivalent circuit for ZCT operation of S_1 .

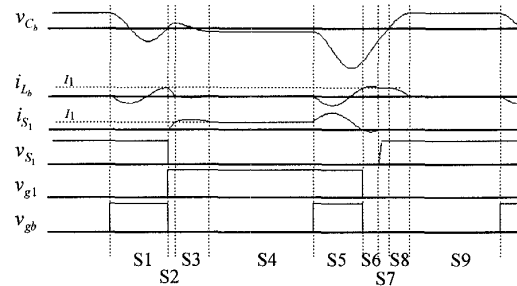


Fig. 14. Key waveforms for S_1 .

4. SIMULATION RESULTS

The PSpice-simulated waveforms of single-pulse and chopping modes for both ZVT and ZCT converters are shown in Figs. 15 to 18, respectively, they closely agree with those theoretical waveforms. The main switches and diodes of the proposed ZVT converter (S_m , D_m and S_1 , D_1) can always maintain ZVS operation. For the proposed ZCT converter, both the main and auxiliary switches (S_m , S_a , S_1 , S_b and S_{b1}) can always operate with ZCS.

5. CONCLUSION

A new family of soft-switching converters for SRM drives has been presented. The ZVT type possesses the definite advantages that all main switches and diodes can achieve ZVS when the corresponding device voltage and current stresses are kept at unity. On the other hand, both the main and auxiliary switches of the ZCT type can always maintain ZCS with minimum current / voltage stress. Both converters utilize a simple circuit topology, minimum hardware count and low cost, leading to achieve high power density and high efficiency.

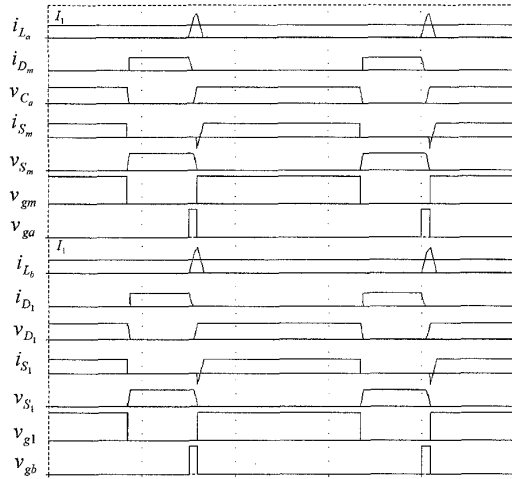


Fig. 15. PSpice simulation showing key waveforms of the ZVT converter (single-pulse mode).

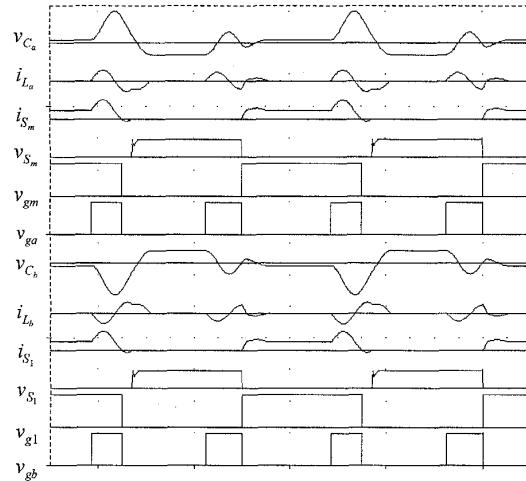


Fig. 17. PSpice simulation showing key waveforms of the ZCT converter (single-pulse mode).

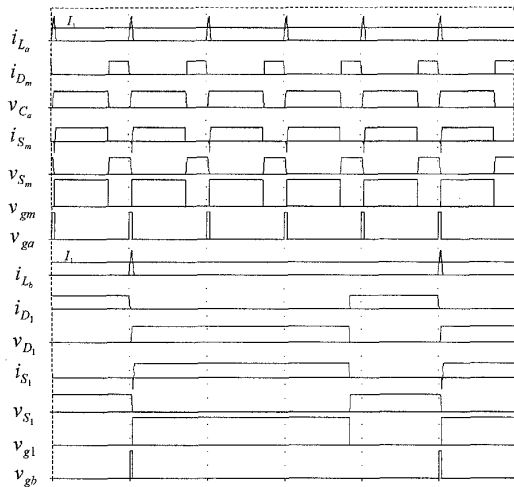


Fig. 16. PSpice simulation showing key waveforms of the ZVT converter (chopping mode).

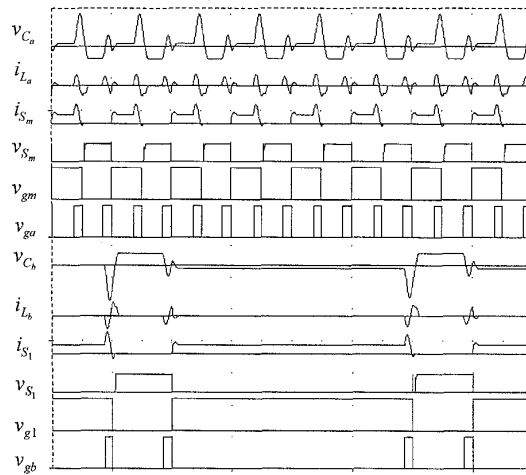


Fig. 18. PSpice simulation showing key waveforms of the ZCT converter (chopping mode).

6. ACKNOWLEDGMENT

This work was supported and funded in part by the Committee on Research and Conference Grants, the University of Hong Kong.

7. REFERENCES

- [1] T.J.E. Miller, "Switched reluctance motors and their control," Magna Physics Publishing, Oxford Science Publications.
- [2] D. Maksimović and S. Čuk, "Constant-frequency control of quasi-resonant converters," *IEEE Trans. Power Electron.*, vol. 6, 1991, pp. 141-150.
- [3] C.C. Chan and K.T. Chau, "A new zero-voltage-switching dc/dc boost converter," *IEEE Trans. Aero. Electron. Syst.*, vol. 29, 1993, pp. 125-134.
- [4] G. Hua, C.S. Leu and F.C. Lee, "Novel zero-voltage-transition PWM converters," In *Proceedings of VPEC Power Electronics Seminar*, 1991, pp. 81-88.
- [5] J.G. Cho, J.W. Baek, G.H. Rim and I. Kang, "Novel zero voltage transition PWM multi-phase converters," In *Proceedings of IEEE APEC*, 1996, pp. 500-506.
- [6] H. Mao, F.C.Y. Lee, X. Zhou, H. Dai, M. Cosan and D. Boroyevich, "Improved zero-current transition converters for high power applications," *IEEE Trans. Ind. Applicat.*, vol. 33, 1997, pp. 1220-1231.
- [7] C.C. Chong, C.Y. Chan and C.F. Foo, "A quasi-resonant converter-fed dc drive system," In *Proceedings of EPE*, 1993, pp. 372-377.
- [8] K.T. Chau, T.W. Ching and C.C. Chan, "Constant-frequency multi-resonant converter-fed dc motor drives," In *Proceedings of IECON*, 1996, pp. 78-83.
- [9] K.T. Chau, T.W. Ching, C.C. Chan and T.W. Chan, "A Novel Soft-Switching Two-Quadrant Converter for DC Motor Drives," In *Proceedings of IECON*, 1997, pp. 517-522.
- [10] Y. Murai, J. Cheng, and M. Yoshida, "A soft-switched reluctance motor drives circuit with improved performances," In *Proceedings of IEEE PESC*, 1997, pp. 881-886.
- [11] J.G. Cho, W.H. Kim, G.H. Rim and, K.Y. Cho, "Novel zero transition PWM converter for switched reluctance motor drives," In *Proceedings of IEEE PESC*, 1997, pp. 887-891.